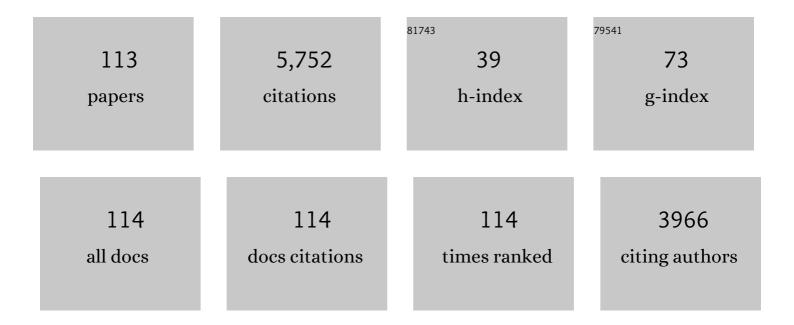
List of Publications by Year in descending order

Source: https://exaly.com/author-pdf/8917782/publications.pdf Version: 2024-02-01



SHAOMINLUL

#	Article	IF	CITATIONS
1	Heihe Watershed Allied Telemetry Experimental Research (HiWATER): Scientific Objectives and Experimental Design. Bulletin of the American Meteorological Society, 2013, 94, 1145-1160.	1.7	705
2	Watershed Allied Telemetry Experimental Research. Journal of Geophysical Research, 2009, 114, .	3.3	295
3	The Heihe Integrated Observatory Network: A Basinâ€Scale Land Surface Processes Observatory in China. Vadose Zone Journal, 2018, 17, 1-21.	1.3	258
4	Intercomparison of surface energy flux measurement systems used during the HiWATERâ€MUSOEXE. Journal of Geophysical Research D: Atmospheres, 2013, 118, 13,140.	1.2	239
5	Differentiating drought legacy effects on vegetation growth over the temperate Northern Hemisphere. Global Change Biology, 2018, 24, 504-516.	4.2	233
6	MODIS-driven estimation of terrestrial latent heat flux in China based on a modified Priestley–Taylor algorithm. Agricultural and Forest Meteorology, 2013, 171-172, 187-202.	1.9	193
7	Hydrological Cycle in the Heihe River Basin and Its Implication for Water Resource Management in Endorheic Basins. Journal of Geophysical Research D: Atmospheres, 2018, 123, 890-914.	1.2	189
8	Upscaling evapotranspiration measurements from multi-site to the satellite pixel scale over heterogeneous land surfaces. Agricultural and Forest Meteorology, 2016, 230-231, 97-113.	1.9	180
9	Validation of remotely sensed evapotranspiration over the Hai River Basin, China. Journal of Geophysical Research, 2012, 117, .	3.3	167
10	Turbulent Flux Transfer over Bare-Soil Surfaces: Characteristics and Parameterization. Journal of Applied Meteorology and Climatology, 2008, 47, 276-290.	0.6	163
11	Evaluating Different Machine Learning Methods for Upscaling Evapotranspiration from Flux Towers to the Regional Scale. Journal of Geophysical Research D: Atmospheres, 2018, 123, 8674-8690.	1.2	141
12	Evaluating parameterizations of aerodynamic resistance to heat transfer using field measurements. Hydrology and Earth System Sciences, 2007, 11, 769-783.	1.9	139
13	Estimation of daily evapotranspiration and irrigation water efficiency at a Landsat-like scale for an arid irrigation area using multi-source remote sensing data. Remote Sensing of Environment, 2018, 216, 715-734.	4.6	120
14	A multiscale dataset for understanding complex eco-hydrological processes in a heterogeneous oasis system. Scientific Data, 2017, 4, 170083.	2.4	109
15	A Method Based on Temporal Component Decomposition for Estimating 1-km All-Weather Land Surface Temperature by Merging Satellite Thermal Infrared and Passive Microwave Observations. IEEE Transactions on Geoscience and Remote Sensing, 2019, 57, 4670-4691.	2.7	97
16	Improving global terrestrial evapotranspiration estimation using support vector machine by integrating three process-based algorithms. Agricultural and Forest Meteorology, 2017, 242, 55-74.	1.9	96
17	Evaluation of twelve evapotranspiration products from machine learning, remote sensing and land surface models over conterminous United States. Journal of Hydrology, 2019, 578, 124105.	2.3	92
18	Monitoring and validating spatially and temporally continuous daily evaporation and transpiration at river basin scale. Remote Sensing of Environment, 2018, 219, 72-88.	4.6	82

#	Article	IF	CITATIONS
19	Application of remote sensing-based two-source energy balance model for mapping field surface fluxes with composite and component surface temperatures. Agricultural and Forest Meteorology, 2016, 230-231, 8-19.	1.9	80
20	Assessment of the Energy Balance Closure under Advective Conditions and Its Impact Using Remote Sensing Data. Journal of Applied Meteorology and Climatology, 2017, 56, 127-140.	0.6	79
21	Integrated hydrometeorological, snow and frozen-ground observations in the alpine region of the Heihe River Basin, China. Earth System Science Data, 2019, 11, 1483-1499.	3.7	79
22	Retrieving high-resolution surface solar radiation with cloud parameters derived by combining MODIS and MTSAT data. Atmospheric Chemistry and Physics, 2016, 16, 2543-2557.	1.9	78
23	Applications of a thermal-based two-source energy balance model using Priestley-Taylor approach for surface temperature partitioning under advective conditions. Journal of Hydrology, 2016, 540, 574-587.	2.3	64
24	Assessment of Uncertainties in Eddy Covariance Flux Measurement Based on Intensive Flux Matrix of HiWATER-MUSOEXE. IEEE Geoscience and Remote Sensing Letters, 2015, 12, 259-263.	1.4	59
25	Mapping regional turbulent heat fluxes via variational assimilation of land surface temperature data from polar orbiting satellites. Remote Sensing of Environment, 2019, 221, 444-461.	4.6	59
26	A LUT-based approach to estimate surface solar irradiance by combining MODIS and MTSAT data. Journal of Geophysical Research, 2011, 116, n/a-n/a.	3.3	56
27	Improving Predictions of Water and Heat Fluxes by Assimilating MODIS Land Surface Temperature Products into the Common Land Model. Journal of Hydrometeorology, 2011, 12, 227-244.	0.7	56
28	Estimating the spatial distribution of soil moisture based on Bayesian maximum entropy method with auxiliary data from remote sensing. International Journal of Applied Earth Observation and Geoinformation, 2014, 32, 54-66.	1.4	53
29	Intercomparison of Six Upscaling Evapotranspiration Methods: From Site to the Satellite Pixel. Journal of Geophysical Research D: Atmospheres, 2018, 123, 6777-6803.	1.2	50
30	Evaluation of SMAP, SMOS-IC, FY3B, JAXA, and LPRM Soil Moisture Products over the Qinghai-Tibet Plateau and Its Surrounding Areas. Remote Sensing, 2019, 11, 792.	1.8	49
31	Physiological and environmental control on ecosystem water use efficiency in response to drought across the northern hemisphere. Science of the Total Environment, 2021, 758, 143599.	3.9	48
32	Temporal Upscaling and Reconstruction of Thermal Remotely Sensed Instantaneous Evapotranspiration. Remote Sensing, 2015, 7, 3400-3425.	1.8	47
33	Estimation of evapotranspiration over the terrestrial ecosystems in China. Ecohydrology, 2014, 7, 139-149.	1.1	45
34	Responses of Water Use Efficiency to Drought in Southwest China. Remote Sensing, 2020, 12, 199.	1.8	45
35	A simple temperature domain twoâ€source model for estimating agricultural field surface energy fluxes from Landsat images. Journal of Geophysical Research D: Atmospheres, 2017, 122, 5211-5236.	1.2	43
36	Rebuilding a Microwave Soil Moisture Product Using Random Forest Adopting AMSR-E/AMSR2 Brightness Temperature and SMAP over the Qinghai–Tibet Plateau, China. Remote Sensing, 2019, 11, 683.	1.8	43

#	Article	IF	CITATIONS
37	Partitioning Evapotranspiration into Soil Evaporation and Canopy Transpiration via a Two-Source Variational Data Assimilation System. Journal of Hydrometeorology, 2016, 17, 2353-2370.	0.7	41
38	Uncertainty analysis of eleven multisource soil moisture products in the third pole environment based on the three-corned hat method. Remote Sensing of Environment, 2021, 255, 112225.	4.6	41
39	Estimations of Regional Surface Energy Fluxes Over Heterogeneous Oasis–Desert Surfaces in the Middle Reaches of the Heihe River During HiWATER-MUSOEXE. IEEE Geoscience and Remote Sensing Letters, 2015, 12, 671-675.	1.4	40
40	Estimating turbulent fluxes through assimilation of geostationary operational environmental satellites data using ensemble Kalman filter. Journal of Geophysical Research, 2011, 116, .	3.3	39
41	Uneven winter snow influence on tree growth across temperate China. Global Change Biology, 2019, 25, 144-154.	4.2	39
42	Evaluation of three complementary relationship approaches for evapotranspiration over the Yellow River basin. Hydrological Processes, 2006, 20, 2347-2361.	1.1	38
43	Quantification of the Scale Effect in Downscaling Remotely Sensed Land Surface Temperature. Remote Sensing, 2016, 8, 975.	1.8	37
44	Estimation of net surface shortwave radiation from MODIS data. International Journal of Remote Sensing, 2012, 33, 804-825.	1.3	34
45	Exploring evapotranspiration changes in a typical endorheic basin through the integrated observatory network. Agricultural and Forest Meteorology, 2020, 290, 108010.	1.9	34
46	Characterizing the Footprint of Eddy Covariance System and Large Aperture Scintillometer Measurements to Validate Satellite-Based Surface Fluxes. IEEE Geoscience and Remote Sensing Letters, 2015, 12, 943-947.	1.4	33
47	Downscaling of surface air temperature over the Tibetan Plateau based on DEM. International Journal of Applied Earth Observation and Geoinformation, 2018, 73, 136-147.	1.4	32
48	Estimation of Regional Evapotranspiration by TM/ETM+ Data over Heterogeneous Surfaces. Photogrammetric Engineering and Remote Sensing, 2007, 73, 1169-1178.	0.3	31
49	Validation and Performance Evaluations of Methods for Estimating Land Surface Temperatures from ASTER Data in the Middle Reach of the Heihe River Basin, Northwest China. Remote Sensing, 2015, 7, 7126-7156.	1.8	29
50	A new model for the automatic relative radiometric normalization of multiple images with pseudo-invariant features. International Journal of Remote Sensing, 2016, 37, 4554-4573.	1.3	27
51	Satellite-Based Analysis of Evapotranspiration and Water Balance in the Grassland Ecosystems of Dryland East Asia. PLoS ONE, 2014, 9, e97295.	1.1	26
52	Validation of Regional-Scale Remote Sensing Products in China: From Site to Network. Remote Sensing, 2016, 8, 980.	1.8	25
53	Assessment and simulation of global terrestrial latent heat flux by synthesis of CMIP5 climate models and surface eddy covariance observations. Agricultural and Forest Meteorology, 2016, 223, 151-167.	1.9	25
54	The characteristics and parameterization of aerodynamic roughness length over heterogeneous surfaces. Advances in Atmospheric Sciences, 2009, 26, 180-190.	1.9	24

#	Article	IF	CITATIONS
55	Upscaling Sensible Heat Fluxes With Area-to-Area Regression Kriging. IEEE Geoscience and Remote Sensing Letters, 2015, 12, 656-660.	1.4	24
56	Estimation of Turbulent Heat Fluxes by Assimilation of Land Surface Temperature Observations From GOES Satellites Into an Ensemble Kalman Smoother Framework. Journal of Geophysical Research D: Atmospheres, 2018, 123, 2409-2423.	1.2	24
57	Mapping regional evapotranspiration in cloudy skies via variational assimilation of all-weather land surface temperature observations. Journal of Hydrology, 2020, 585, 124790.	2.3	24
58	A Bayesian Three-Cornered Hat (BTCH) Method: Improving the Terrestrial Evapotranspiration Estimation. Remote Sensing, 2020, 12, 878.	1.8	24
59	Evapotranspiration partitioning for multiple ecosystems within a dryland watershed: Seasonal variations and controlling factors. Journal of Hydrology, 2021, 598, 126483.	2.3	24
60	Study on NDVI-T s space by combining LAI and evapotranspiration. Science in China Series D: Earth Sciences, 2006, 49, 747-754.	0.9	22
61	Evaluation of EDI derived from the exponential evapotranspiration model for monitoring China's surface drought. Environmental Earth Sciences, 2011, 63, 425-436.	1.3	22
62	Estimating and Validating Soil Evaporation and Crop Transpiration During the HiWATER-MUSOEXE. IEEE Geoscience and Remote Sensing Letters, 2015, 12, 334-338.	1.4	21
63	Continuous evaluation of the spatial representativeness of land surface temperature validation sites. Remote Sensing of Environment, 2021, 265, 112669.	4.6	21
64	A dual-pass data assimilation scheme for estimating surface fluxes with FY3A-VIRR land surface temperature. Science China Earth Sciences, 2015, 58, 211-230.	2.3	20
65	Satellite detection of increases in global land surface evapotranspiration during 1984–2007. International Journal of Digital Earth, 2012, 5, 299-318.	1.6	19
66	Weakening Relationship Between Vegetation Growth Over the Tibetan Plateau and Largeâ€6cale Climate Variability. Journal of Geophysical Research G: Biogeosciences, 2018, 123, 1247-1259.	1.3	19
67	Impact of Lake/Reservoir Expansion and Shrinkage on Energy and Water Vapor Fluxes in the Surrounding Area. Journal of Geophysical Research D: Atmospheres, 2020, 125, e2020JD032833.	1.2	18
68	Applications of a thermal-based two-source energy balance model coupled to surface soil moisture. Remote Sensing of Environment, 2022, 271, 112923.	4.6	18
69	Evaluation of a satellite-derived model parameterized by three soil moisture constraints to estimate terrestrial latent heat flux in the Heihe River basin of Northwest China. Science of the Total Environment, 2019, 695, 133787.	3.9	17
70	Preliminary validation of GLASS-DSSR products using surface measurements collected in arid and semi-arid regions of China. International Journal of Digital Earth, 2013, 6, 50-68.	1.6	16
71	Evaluation of the Weak Constraint Data Assimilation Approach for Estimating Turbulent Heat Fluxes at Six Sites. Remote Sensing, 2018, 10, 1994.	1.8	16

5

#	Article	IF	CITATIONS
73	Improve the Performance of the Noahâ€MP rop Model by Jointly Assimilating Soil Moisture and Vegetation Phenology Data. Journal of Advances in Modeling Earth Systems, 2021, 13, e2020MS002394.	1.3	15
74	Using the Surface Temperature-Albedo Space to Separate Regional Soil and Vegetation Temperatures from ASTER Data. Remote Sensing, 2015, 7, 5828-5848.	1.8	14
75	Estimation of surface heat fluxes using multi-angular observations of radiative surface temperature. Remote Sensing of Environment, 2020, 239, 111674.	4.6	14
76	Scaling Flux Tower Observations of Sensible Heat Flux Using Weighted Area-to-Area Regression Kriging. Atmosphere, 2015, 6, 1032-1044.	1.0	13
77	Investigating microclimate effects in an oasis-desert interaction zone. Agricultural and Forest Meteorology, 2020, 290, 107992.	1.9	13
78	A Satellite-Based Method for National Winter Wheat Yield Estimating in China. Remote Sensing, 2021, 13, 4680.	1.8	13
79	Estimating Corn Canopy Water Content From Normalized Difference Water Index (NDWI): An Optimized NDWI-Based Scheme and Its Feasibility for Retrieving Corn VWC. IEEE Transactions on Geoscience and Remote Sensing, 2021, 59, 8168-8181.	2.7	12
80	Upscaling Evapotranspiration from a Single-Site to Satellite Pixel Scale. Remote Sensing, 2021, 13, 4072.	1.8	12
81	Improving predictions of evapotranspiration by integrating multi-source observations and land surface model. Agricultural Water Management, 2022, 272, 107827.	2.4	12
82	Wind Dynamics Over a Highly Heterogeneous Oasis Area: An Experimental and Numerical Study. Journal of Geophysical Research D: Atmospheres, 2018, 123, 8418-8440.	1.2	11
83	Component radiative temperatures over sparsely vegetated surfaces and their potential for upscaling land surface temperature. Agricultural and Forest Meteorology, 2019, 276-277, 107600.	1.9	11
84	Merging the MODIS and Landsat Terrestrial Latent Heat Flux Products Using the Multiresolution Tree Method. IEEE Transactions on Geoscience and Remote Sensing, 2019, 57, 2811-2823.	2.7	11
85	Satellite Detection of Water Stress Effects on Terrestrial Latent Heat Flux With MODIS Shortwave Infrared Reflectance Data. Journal of Geophysical Research D: Atmospheres, 2018, 123, 11,410.	1.2	10
86	Mapping Regional Turbulent Heat Fluxes via Assimilation of MODIS Land Surface Temperature Data into an Ensemble Kalman Smoother Framework. Earth and Space Science, 2019, 6, 2423-2442.	1.1	10
87	Estimation of Daily Terrestrial Latent Heat Flux with High Spatial Resolution from MODIS and Chinese GF-1 Data. Sensors, 2020, 20, 2811.	2.1	10
88	Assessment and improvement of Noah-MP for simulating water and heat exchange over alpine grassland in growing season. Science China Earth Sciences, 2022, 65, 536-552.	2.3	9
89	Applying a Wavelet Transform Technique to Optimize General Fitting Models for SM Analysis: A Case Study in Downscaling over the Qinghai–Tibet Plateau. Remote Sensing, 2022, 14, 3063.	1.8	9
90	Application of ensemble kalman filter to geophysical parameters retrieval in remote sensing: A case study of kernel-driven BRDF model inversion. Science in China Series D: Earth Sciences, 2006, 49, 632-640.	0.9	8

#	Article	IF	CITATIONS
91	Evaluating Spatial Heterogeneity of Land Surface Hydrothermal Conditions in the Heihe River Basin. Chinese Geographical Science, 2020, 30, 855-875.	1.2	8
92	Modeling Transpiration with Sun-Induced Chlorophyll Fluorescence Observations via Carbon-Water Coupling Methods. Remote Sensing, 2021, 13, 804.	1.8	8
93	A long-term 0.01° surface air temperature dataset of Tibetan Plateau. Data in Brief, 2018, 20, 748-752.	0.5	6
94	Micrometeorological Methods to Determine Evapotranspiration. Ecohydrology, 2018, , 1-39.	0.2	5
95	Estimation of Turbulent Heat Fluxes and Gross Primary Productivity by Assimilating Land Surface Temperature and Leaf Area Index. Water Resources Research, 0, , .	1.7	5
96	Correction to "A Method Based on Temporal Component Decomposition for Estimating 1-km All-Weather Land Surface Temperature by Merging Satellite Thermal Infrared and Passive Microwave Observations―[Feb 19 4670-4691]. IEEE Transactions on Geoscience and Remote Sensing, 2019, 57, 6254-6254.	2.7	3
97	Diagnosing the Temperature Sensitivity of Ecosystem Respiration in Northern High‣atitude Regions. Journal of Geophysical Research G: Biogeosciences, 2021, 126, e2020JG005998.	1.3	3
98	Simulating Airflow Around Flexible Vegetative Windbreaks. Journal of Geophysical Research D: Atmospheres, 2021, 126, e2021JD034578.	1.2	3
99	Reconstruction of remotely sensed daily evapotranspiration data in cloudy-sky conditions. Agricultural Water Management, 2021, 255, 107000.	2.4	3
100	Improvements in land surface temperature retrieval based on atmospheric water vapour content and atmospheric temperature. International Journal of Remote Sensing, 2014, 35, 4881-4904.	1.3	2
101	A Parameterized Multiangular Microwave Emission Model of L-, C-, and X-Bands for Corn Considering Multiple-Scattering Effects. IEEE Geoscience and Remote Sensing Letters, 2018, 15, 1249-1253.	1.4	2
102	Integrating Latent Heat Flux Products from MODIS and Landsat Data Using Multi-Resolution Kalman Filter Method in the Midstream of Heihe River Basin of Northwest China. Remote Sensing, 2019, 11, 1787.	1.8	2
103	An intercomparison study on models of estimating the aerodynamic resistance. , 0, , .		1
104	Comparison of different complementary relationship models for estimating regional evapotranspiration. , 0, , .		1
105	Intercomparison of evapotranspiration models using remote sensing date and ground measurements during the MUSOEXE-12 campaign. , 2013, , .		1
106	A framework for validating remotely sensed evapotranspiration. , 2016, , .		1
107	Micrometeorological Methods to Determine Evapotranspiration. Ecohydrology, 2018, , 1-39.	0.2	1

0

#	Article	IF	CITATIONS
109	A simple interpretation of NDVI-Ts space combining LAI and evapotranspiration. , 0, , .		0
110	Estimation of regional evapotranspiration in the mu us sandland. , 0, , .		0
111	A study of soil heat flux. , 0, , .		0
112	Micrometeorological Methods to Determine Evapotranspiration. Ecohydrology, 2019, , 201-239.	0.2	0
113	Application of the two-source energy balance model with microwave-derived soil moisture in a semi-arid agricultural region. International Journal of Applied Earth Observation and Geoinformation, 2022, 112, 102879.	0.9	0